https://doi.org/10.48048/tis.2023.6978

Evaluation of Toxic Heavy Metals and Health Risk in Airborne Particulate Matter at Qassim region, Saudi Arabia

Hamed Alnagran[1,2], Howaida Mansour[3,4], Saleh Alashrah[2], Nursakinah Suardi[1,*] and Azhar Abdul Rahman[1]

[1]School of Physics, Universiti Sains Malaysia, 11800 Penang, Malaysia
[2]Physics Department, College of Science, Qassim University, Buraydah 51452, Saudi Arabia
[3]Physics Department, College of Science and Art, Qassim University, Ar Rass 51921, Saudi Arabia
[4]Physics Department, Faculty of Women for Arts, Science and Education, Ain Shams University, Cairo 11757, Egypt

([*]Corresponding author's e-mail: nsakinahsuardi@usm.my)

Received: 11 April 2023, Revised: 15 May 2023, Accepted: 18 May 2023, Published: 28 August 2023

Abstract

Particulate matter (PM) significantly influences air quality, visibility, climate change, the earth's radiative balance, and human health. The significance of carrying out this investigation in its entirety is due to the small amount of data that has been collected and published in Qassim region (26.2078º N, 43.4837º E). Understanding the origins of PM and its chemical species in Qassim districts is advantageous for the purpose of identifying impacts on one's health Characterization of pollution sources also will assist in the success of mitigation strategies and solve the issue of increased PM concentrations in outdoor areas. Therefore, this study described the physical and chemical properties of PM by measuring the PM_1, $PM_{2.5}$, and PM_{10} concentrations in Qassim's central urban and rural areas. In urban Qassim, the average PM_1, $PM_{2.5}$, and PM_{10} concentrations were 12.23, 33.16, and 155.38 μg/m^3, respectively. On the other hand, the average PM_1, $PM_{2.5}$, and PM_{10} concentrations reached 8.18, 23.03, and 93.57 μg/m^3 in rural Qassim, respectively. The findings revealed that fine particle concentrations have risen over allowable levels due to dust storms. A total of 18 elements and 8 chemical compounds were determined and identified. The compound concentrations of Al_2O_3, SiO_2, CaO, TiO_2, K_2O, BaO, MnO, Fe_2O_3 and the essential elements Sr, V, Al, Cu, Ca, Fe, Cr, As, Zr, K, Br, Ba, Pb, Mn, Ni, Zn, Rb and Ti were determined using XRF and XRD. The findings revealed that fine particle concentrations have risen over allowable levels due to dust storms. The main elements in the trace elements were Ca, Fe, Al, Sr, K, and Mg, indicating significant contributions from the soil (Ca, Fe, Al, Mg), as well as from industrial and vehicle emissions (Sr, Ca, Al, Fe, K). V, Cu, Zn, Cr, Ni, Pb, Sr, As, Mn and Br fall under the anthropogenic category of trace elements, while Al, S, Na, Mg, Rb, K, Zr, Ti, Fe, Mn, Sr, Y, Cr, Ca, Ni, Zn and Cu are obtained from the earth's crust.

Keywords: PM, Airborne, Air quality, PM monitoring, Concentration, Chemical analysis, Metals, Pollution, Air quality, Qassim, Saudia Arabia

Introduction

Airborne particulate matter (PM) contaminants play a major role in the transmission of microbial, infectious, and allergic diseases which may induce or enhance respiratory disorders [1,2]. PM affects the air quality and in turn, the well-being of humans and ecosystems [3,4]. A recent study of the Qassim area revealed the marked rise (from 7.1 to 15.7 %) in the total prevalence rate of non-communicable diseases, such as cardiovascular diseases and complications with the eye and skin, between 2011 and 2015. These increases in the prevalence of illnesses were ascribed to air pollution and high PM level [5]. The health symptoms aggravated as the number of sandstorms increased due to low pressure in the north of Qassim in spring, the incidences of sandstorms have increased. Sandstorms are sparked by cold fronts in such low-pressure regions. Dust particles are dispersed due to the approaching 20 km/h horizontal wind speed. The majority of dust storms occur when velocity exceeds 35 km/h [6]. Because of Saudi Arabia's typical semi-arid to dry environment, air pollutants linger in the atmosphere for a longer period of time. While sandstorms are a significant contributor to air pollution in Saudi Arabia, several studies [7-9] have revealed a significant contribution from anthropogenic emissions, particularly those related to the combustion of fossil fuels and vehicle emissions. Thus, additional air quality tests are required in Saudi Arabia's main cities.

Given the physical and chemical properties of the atmosphere, around half of the elements in airborne PM exist largely in the crust and are possibly derived from soil. Deserts are potentially the central origin of this crustal dust in distant temperate and polar zones [10-12]. The size, shape, and chemical composition of PM are regarded to be the key variables in human toxicity, with smaller particles being more harmful than the same mass of large particles when all other criteria are equal [13]. Furthermore, it has been proposed that low-toxicity results are produced from soil dust, sodium chloride, and ammonium nitrate, despite the fact that they constitute the majority of the continental border layer of $PM_{2.5}$ mass concentrations [14]. In contrast, transition metals, which account for a small proportion of total $PM_{2.5}$ mass concentration, are assumed to be very hazardous [15]. As a result, understanding PM composition in depth can aid in toxicity assessment and enable policies to target emission sources associated with the most harmful components in order to most effectively mitigate the health implications of poor air quality.

The Qassim Region, which is located in the Kingdom of Saudi Arabia, is home to a variety of different types of PM, the most common of which include marine, desert, and anthropogenic particles. The physical position of the nation, which is sandwiched between the Arabian Gulf and extensive desert regions, is largely responsible for the prevalence of the first 2 categories. Quartz, calcite, dolomite, feldspars, gypsum, and clay minerals are the primary components of marine aerosols, while quartz, calcite, dolomite, feldspars, and gypsum are the primary components of desert PM. Marine aerosols are produced by the spray of the Arabian Gulf [16,17]. The emissions of industrial processes, the creation of electrical power, and agricultural practices all contribute to the production of anthropogenic aerosols. During the course of the last several decades, for example, the investigation of the amount of metals found in PM and the impact of PM has captured the interest of a number of researchers; in the area, for example, a comprehensive study was carried out in Kuwait [18-22] and Emirates [23-27].

In addition, industrial pollution, the production of energy, and farming activities produce anthropogenic PM. Over the last several decades, several researchers have studied the metal contents of dust and the influence of PM on the environment; the survey findings revealed the increased contamination of PM within a short period of time (1 year) [28-30].

Environmental PM is not only an individual pollutant but also consists of various chemical species, including trace metals, elemental carbon, nitrate, sulphates, and various organic species [31]. The chemical components of PM are typically measured at government agency-established fixed testing stations, which are operated for regulatory purposes. However, in Qassim, Saudi Arabia, no data are available because chemical components are not assessed by tracking networks. Additionally, there are not enough data available for measurements of particle concentration.

Therefore, the aim of this research was to study the concentrations of atmospheric PM (PM_1, $PM_{2.5}$, and PM_{10}) and finding out what elements are in airborne PM samples and evaluate the extent of quantification as well of the particles suspended in the medium filter at 23 locations in the Qassim region. On the basis of the mass concentrations of PM and its chemical components, including chemical compound and trace elements, we provide a complete evaluation and delineation of numerous emission sources of particle (PM) air pollution in Qassim. This study will provide an overview of the air quality and contribute to our understanding of the features of particulate matter in this area of the world. Furthermore, the information obtained from this research will fill the gap in the scarcity of data on particles in this region. In addition, the findings of this study are essential for guiding the development and application of the current policies for the prevention of air pollution in Qassim and the rest of Saudi Arabia.

Materials and methods

Location description

Qassim is one of Saudi Arabia's 13 administrative districts, located in the middle of the region. The hot season lasted for 4 - 5 months, with a daily high temperature above 40 ºC, from May 2019 to September 2020. The winter season lasted for 3 months, and the maximum temperatures were below 25 ºC daily between November 26 and February 26.

Qassim is the seventh most populous zone in the country, with a population of 1,016,756 [32] and an area of 58,046 km^2. It is considered the country's "food bowl" due to its agricultural riches. The Qassim area has a typical desert climate and is known for its cold, rainy winters, and dry, less humid summers. On January 19, the highest rainfall starts, and this condition lasts for 1 month; the total overall precipitation is 8 mm. At the beginning of July, the minimum rainfall is ~0 mm. The primary causes of PM emissions in Qassim comprise farm waste and heavy road traffic. Occasionally, dust storms occur from March to September, but they can be observed at any time of the year. The wind speed and direction vary considerably more than the hourly average. It is calculated as the wide-scale wind vector average at 10 m

above the ground. The average annual wind speed is 4.2 m/s from January to August [33]. However, the low wind intensity remains at an average of 5.6 months, that is, from August to January, at a rate of 3.5 m/s. The humidity level in Qassim remains constant during the year. Samples were collected from 23 locations that represent urban cities in the Qassim region during different seasons from May 2019 to September 2020. **Figure 1** and **Table 1** show the position of the sampling site. **Figure 2** illustrates the mean temperature in the Qassim region.

Figure 1 Geological map of the studied PM in Qassim region [34,35].

Table 1 Locations of the samples collected.

Sample	Location (City)
S1	North Alrass
S2	Centre Alrass
S3	South Alrass
S4	North Buraydah
S5	Centre Buraydah
S6	South Buraydah
S7	Alshmasiyah
S8	Alrubayiyah
S9	North Unizah
S10	Centre Unizah
S11	South Unizah
S12	Albukayriyah
S13	Almalida
S14	Albadayea
S15	Alhilaliah
S16	Riyadh Alkhabra
S17	Alkhabra
S18	Alfuwayliq
S19	UyunAljawa
S20	UglatAsugour
S21	Almithnab
S22	Alnabhaniyah
S23	Alasyah

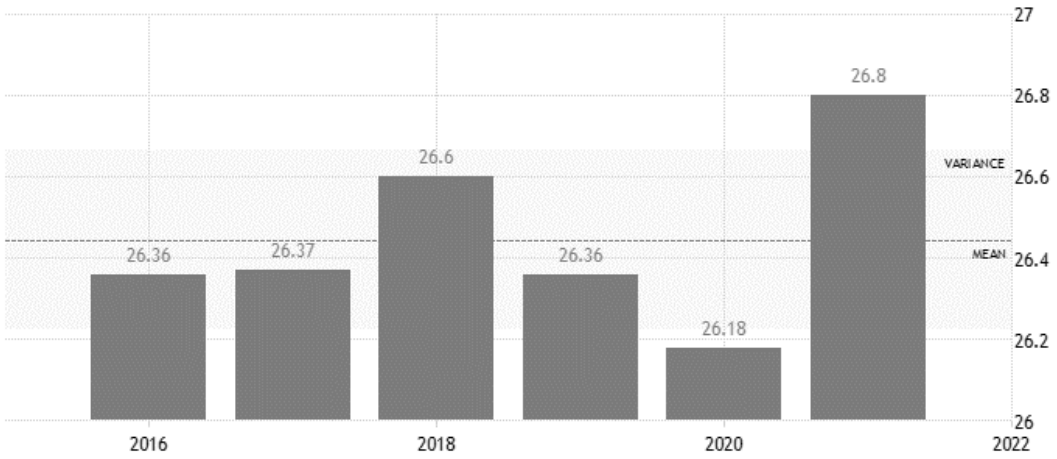

Figure 2 Mean temperature (observed data) for the Qassim region (6 years) [36].

Sample collection and preparation

A total of 276 samples were collected for the purpose of conducting chemical analysis from 23 different locations in Qassim. Before the initial phase of measurement, each sample was held in a plastic bag and homogenized (i.e., thoroughly mixed by stirring and rotating). All samples were measured in triplicate. **Figure 3** shows the device used to collect PM samples for the project. The device consisted of a pipe housing (60 cm (length) × 47 mm (diameter)) with a Teflon-membrane and quartz fiber filters mounted in the middle with a polysynthetic membrane (47 mm diameter) axial extract fan. During collection, the instrument was placed 1.5 m above ground level. The samples were sieved using a 0.125 mm sieve to remove ash (bark and compound leaves). The model sampling device collected particles at acceptable ($d < 2.5$ µm) and field ($2.5 < d < 10$ µm) flow rates of 35 m^3/h, where d represents the diameter of particles.

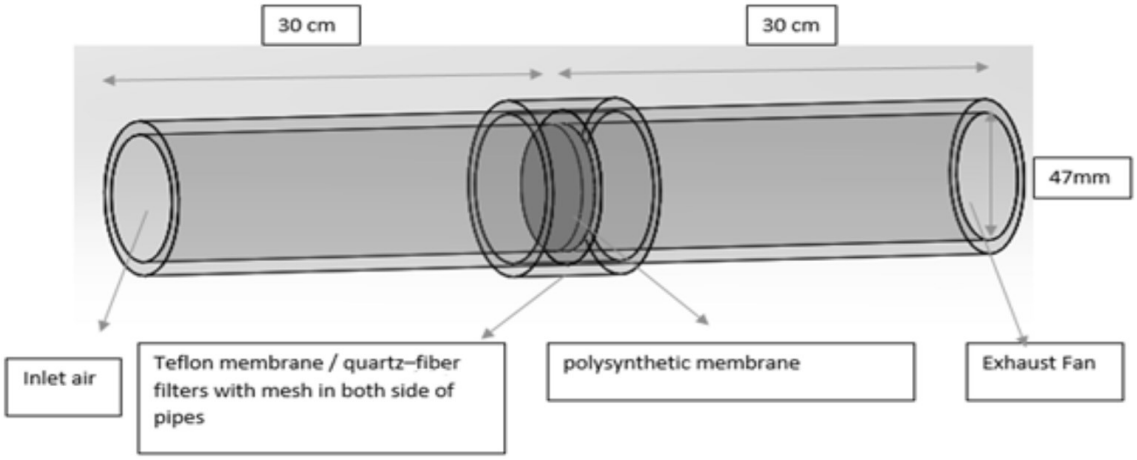

Figure 3 Device used for sample collections.

PM monitoring

Two dust detectors (Grimm Spectrometer Particles, Model 1.108, Germany; aerosol spectrometer and dust monitor) were used to measure the concentrations and proportions of particle sizes from 1 µg m^{-3} to 100 µg m^{-3}, with a minimal detectable particle size of 0.75 µm. PM concentrations were measured in urban and rural areas, and their differences were compared.

The monitoring of PM was conducted at 2 locations: The city center of Buraydah on King Abdulaziz Road for the urban area and another location at the Qassim University campus for the rural area. The Grimm Spectrometer Particles (detector) were placed 7 m above the ground. Air quality monitoring was carried out at these locations for one year, that is, from July 2020 to June 2021.

Chemical analysis techniques

The chemical composition of PM will decide the form and severity of toxic reactions because different metals and organic compounds influence environmental and health effects of particles [37,38]. In this study, X-ray fluorescence (XRF) and X-ray diffraction (XRD) were used to analyze the samples.

The ARL Quant'X (Thermo Scientific Inc., USA) energy-dispersive XRF (EDXRF) instrument was used at Qassim University Laboratory to analyze the samples. A total of 18 elements, including Ca, Al, Fe, K, Sr, Ti, V, Cr, Mn, Zr, Ni, Cu, Zn, Pb, As, Ba, Rb, and Br, have been considered in the EDXRF study to obtain accurate quantitative details quickly. The metal composition of each sample was determined.

XRD (Rigaku, UK) analysis was used to determine the crystalline phases in the substances and discover details about their chemical composition by observing the crystalline structure. Phases were identified by matching the data obtained with the information retrieved in comparison databases.

Enrichment coefficient

The relative abundances of numerous elements in the atmospheric PM are regulated by crustal aerosol. Enrichment factor (EF) analysis, which determines the normalized EF of each element in the PM compared with the crust, best demonstrates this phenomenon. EF analysis is often performed for an element using Eq. (1) [39-41].

$$EF = \frac{\left(\frac{C_x}{C_{Fe}}\right)_{PM}}{\left(\frac{C_x}{C_{Fe}}\right)_{crust}} \quad (1)$$

where $\left(\frac{C_x}{C_{Fe}}\right)_{PM}$ is the ratio of an element's content to Fe content in the sample, and $\left(\frac{C_x}{C_{Fe}}\right)_{crust}$ denotes the ratio of the same reference or background element; in this example, Fe originated from the upper continental crust (UCC), according to Rudnick and Gao [42]. The degree of contamination was measured using the interpretive categories proposed by Ganor *et al.* [16].

Result and discussion

Physical analysis results

The average particle concentrations in urban and rural areas were measured from July 2020 to June 2021 are shown in **Figures 4** and **5**. The PM concentrations in March, April, June, August, and May were higher than those in December, January, February, October, and September.

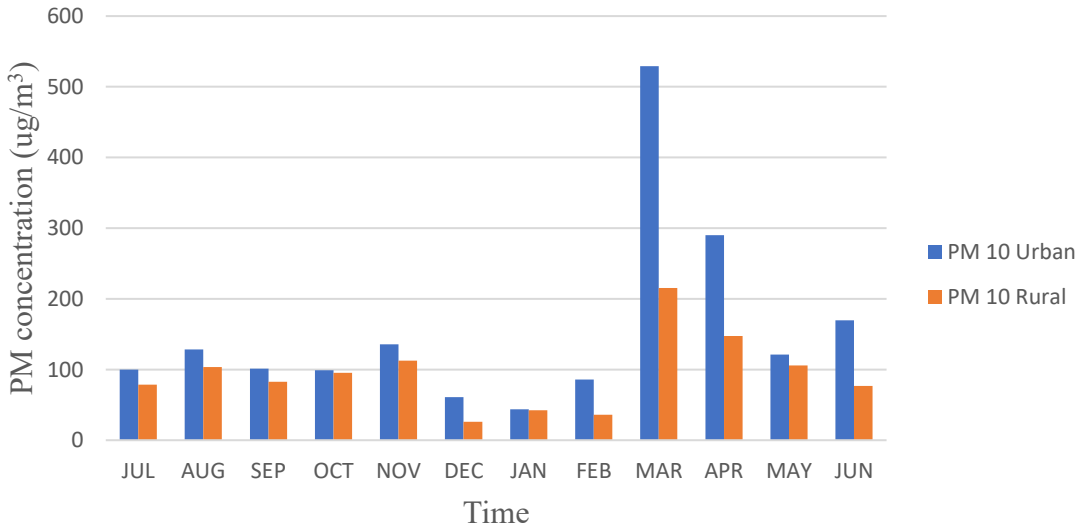

Figure 4 Comparisons of PM_{10} concentration in urban and rural areas.

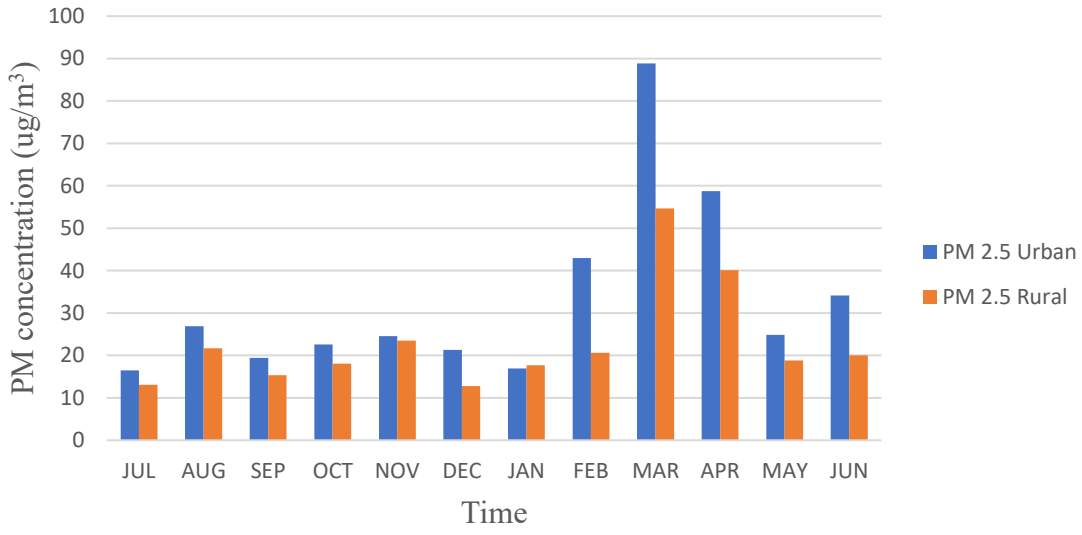

Figure 5 Comparison of $PM_{2.5}$ concentrations in urban and rural areas.

Table 2 Comparison of Average PM concentration in different locations.

Location	PM $_{2.5}$ µg/m^3	PM_{10} µg/m^3	Reference
Present study	32.79	151.67	-
Saudi Arabia	87.90	NA	[43]
Damam, Saudi Arabia	89	NA	[44]
Makkah, Saudi Arabia	84.2	NA	[45]
Jeddah, Saudi Arabia	28.4	87.3	[46]
Beirut, Lebanon	33.1	51.3	[47]
Doha, Qatar	40	145	[48]
Qena, Egypt	NA	114.32	[49]

Average PM concentrations of PM_{10} and $PM_{2.5}$ in urban area within 1 year is 151.67 and 32.79 µg/m^3, respectively. While in rural area PM concentrations of PM_{10} and $PM_{2.5}$ is 93.57 and 23.03 µg/m^3, respectively. These values are higher by multiple times compared with those in the USA (2 - 27 µg/m^3 for $PM_{2.5}$ and 2 - 35 µg/m^3 for PM_{10}) [50] and Europe (7 - 39 µg/m^3 for $PM_{2.5}$ and 8 - 55 µg /m^3 for PM_{10}) [51]. **Table 2** compared PM concentration in different locations, these present values are lower compared with those in Damam, Makkah, and Qatar for $PM_{2.5}$. There are similar values in $PM_{2.5}$ concentration in Qassim, Jeddah and Lebanon. The PM_{10} in Qassim is higher compared with those in Jeddah, Qatar, Egypt and Lebanon. The significant reasons are likely attributable to high PM levels in Saudi Arabia, which is known for its dust storms and oil companies. Notably, the PM concentration constantly decreased, but the levels rose sharply, creating a peak representing the sandstorm effects on (from March to August). The findings also indicate the disparity between day and night readings, where concentrations were reduced at night (**Figure 6**). At 1 Am and 1 Pm, the wind speed is higher, which raises the PM concentration in rural compared to urban and this represents the peak in **Figure 6**.

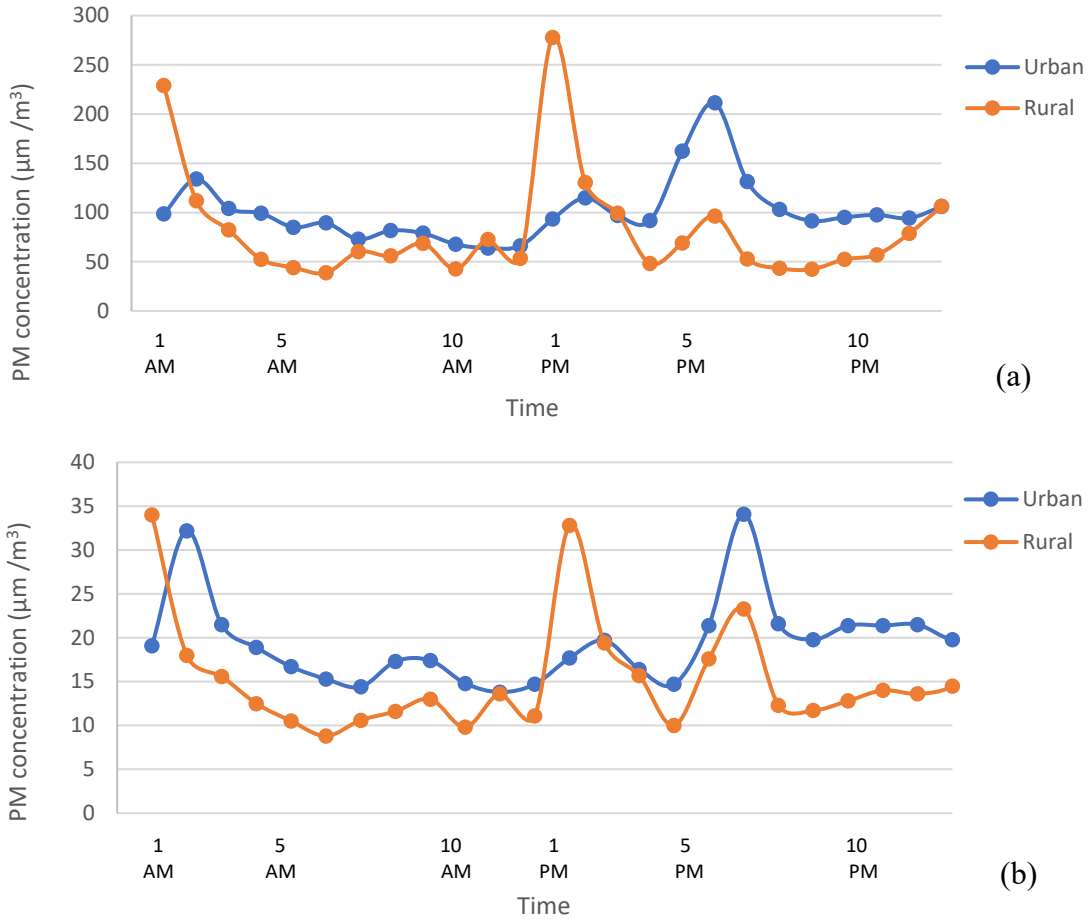

Figure 6 Accumulation of PM in urban and rural areas ((a) PM_{10} and (b) $PM_{2.5}$) and the disparity between day and night readings.

Moreover, the concentrations during sandstorms (from May to August) have reached a maximum level that exceeds the standard limits stipulated by the World Health Organization [52] and the Presidency of Meteorology and Environment (PME) of Saudi Arabia regulates $PM_{2.5}$ at 15 and 35 µg/m^3 annual and 24-h mean, respectively, that is, 500 µg/m^3 for the PM_{10} concentrations and 800 µg/m^3 for the $PM_{2.5}$ concentrations. The concentrations remained high for several hours after the storm, which resulted in a major adverse effect on human health. PM irritates the respiratory system causing nose allergies and asthma. PM may cause bacterial conjunctivitis, which occurs as a result of frequent eye exposure to dust [53].

The levels of PM indicated evident differences depending on the season (**Figures 4** and **5**). In spring and summer (March to August), the $PM_{2.5}$ and PM_{10} concentrations were higher than those in autumn and winter (spring to February). The high concentration in summer was due to the impacts of sand and dust storms and dry soil. The lowest amount recorded during winter was due to heavy rainy precipitation. These findings gave a variation of PM_{10} and $PM_{2.5}$ concentrations in urban and rural areas. Urban PM_{10} and $PM_{2.5}$ levels were higher than those in rural areas. In urban areas, PM concentrations can be tens higher than those in the past, suggesting the enormous inhomogeneity of space. The elevated levels in urban areas were attributable to intensive anthropogenic practices, such as transportation and industry [54]. In the comparison, the urban $PM_{2.5}$ level was 32.79 µg/m^3, and the rural $PM_{2.5}$ level was 23.41 µg/m^3. Meanwhile, the urban PM_{10} level was 151.67 µg/m^3, and the rural PM_{10} level was 97.28 µg/m^3.

Figure 7 depicts an example of monitoring particles over a period of 235 hours, which shows the concentration of particles (PM_{10}, $PM_{2.5}$ and PM_1) and the occurrence of a peak during a dust storm.

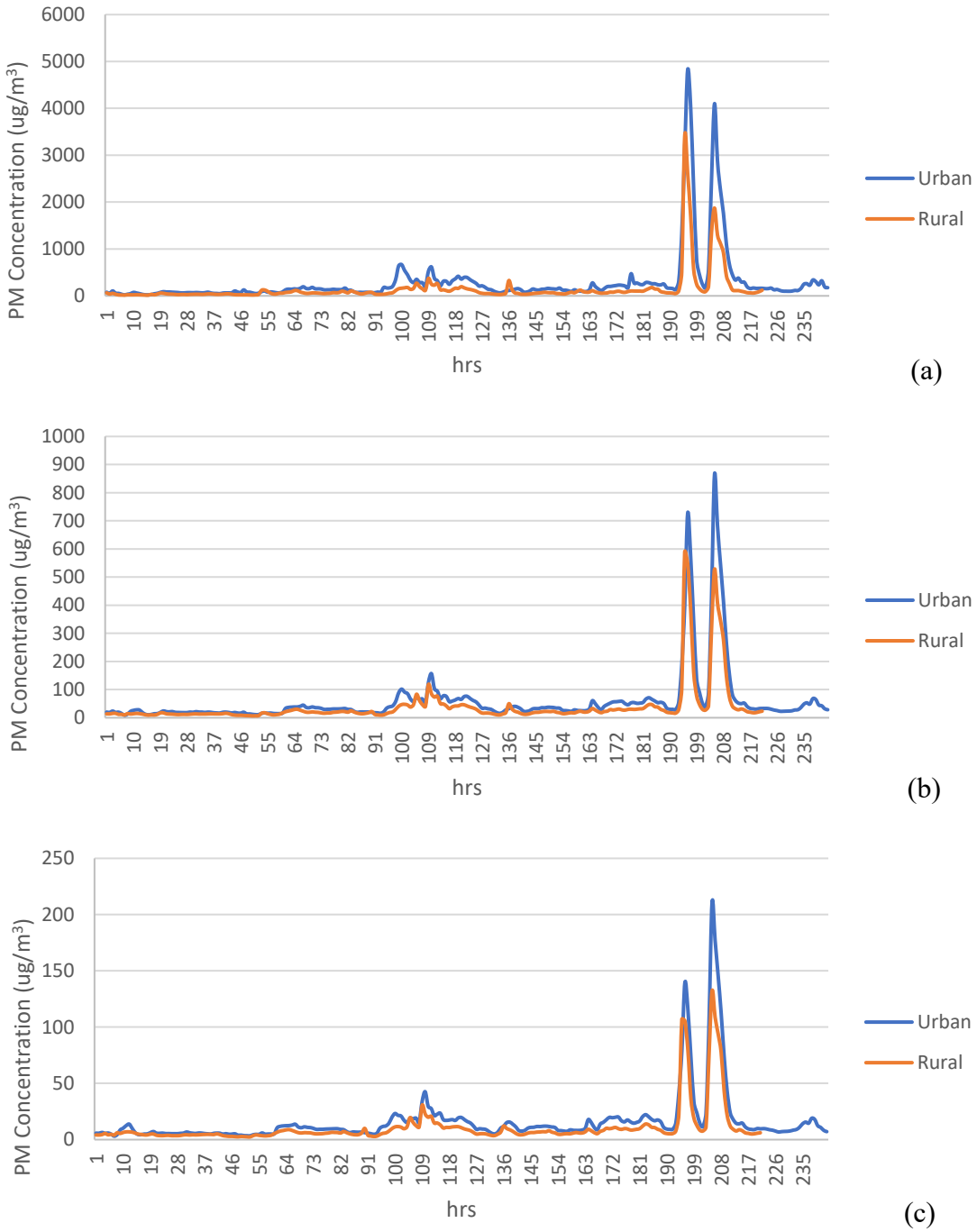

Figure 7 (a) PM_{10}, (b) $PM_{2.5}$ and (c) PM_1 concentrations in urban and rural areas of Qassim.

Chemical analysis results

Table 3 and **Figure 8** present the 18 elements analyzed by EDXRF: Al, V, Cr, Ni, Cu, Ca, Zn, Zr, As, K, Br, Ba, Sr, Rb, Pb, Ti, Mn, and Fe. The chemical compound percentages, including those of SiO_2, $Al2O_3$, CaO, Fe_2O_3, K_2O, TiO_2, MnO, and BaO, were also calculated for each sample (**Tables 3** and **4** and **Figures 8** and **9**). The mentioned elements were selected due to their toxicity and their effect on human health when inhaled. They may lead to death if their concentration is high, and individuals may also be affected by their cumulative effects [55,56].

Table 3 Average chemical abundances of deposition sample.

Elements	Analysis method	Minimum Concentration ppm (mg/kg)	Maximum Concentration ppm (mg/kg)	Average Concentration ppm (mg/kg)	UCC (R and G 2003) ppm (mg/kg)
Al	XRF	16460	28650	22500±380	81500
V	XRF	47	138	90±23	97
Ni	XRF	28	96	59±13	47
Cr	XRF	47	152	102±23.7	92
Fe	XRF	9475	25200	12382±351	39200
Cu	XRF	26	88	50±17	28
Ca	XRF	23458	35600	27876±337	25700
Zn	XRF	36	264	150±60	67
Zr	XRF	69	512	187±97	193
As	XRF	0	12	3±1.8	4.8
K	XRF	2512	9114	4620±187	23200
Br	XRF	12	79	30±17	1.6
Ba	XRF	324	597	443±69	628
Sr	XRF	148	421	249±81	320
Rb	XRF	17	92	40±19	84
Pb	XRF	16	43	26±8	17
Ti	XRF	0.16	0.40	0.32±0.08	0.90
Mn	XRF	159	307	223±47	775

* Average ± STDEV

Table 4 Chemical compound in deposition samples.

Compound	Analysis method	Concentration (%)	UCC (Rudnick and Gao [57])
SiO_2	XRF	36.77±8.9	66.6
Al_2O_3	XRF	3.533±0.8	15.4
CaO	XRF	2.751±1.4	3.59
Fe_2O_3	XRF	4.45±0.9	5.04
K_2O	XRF	0.617±0.18	2.80
TiO_2	XRF	0.542±0.12	0.64
MnO	XRF	0.164±0.07	0.10
BaO	XRF	0.0743±0.013	-

* Average ± STDEV

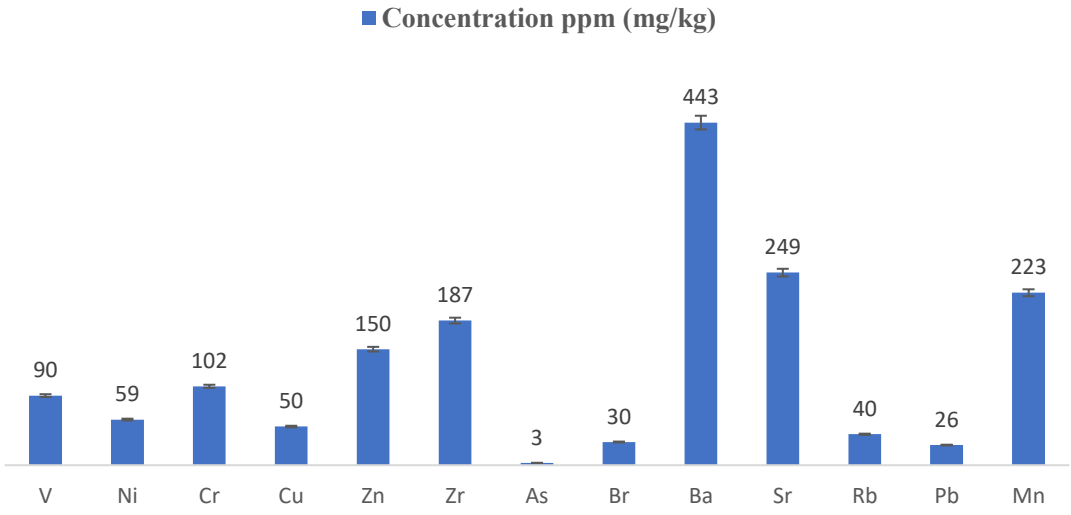

Figure 8 Chemical concentration of deposition samples (elements).

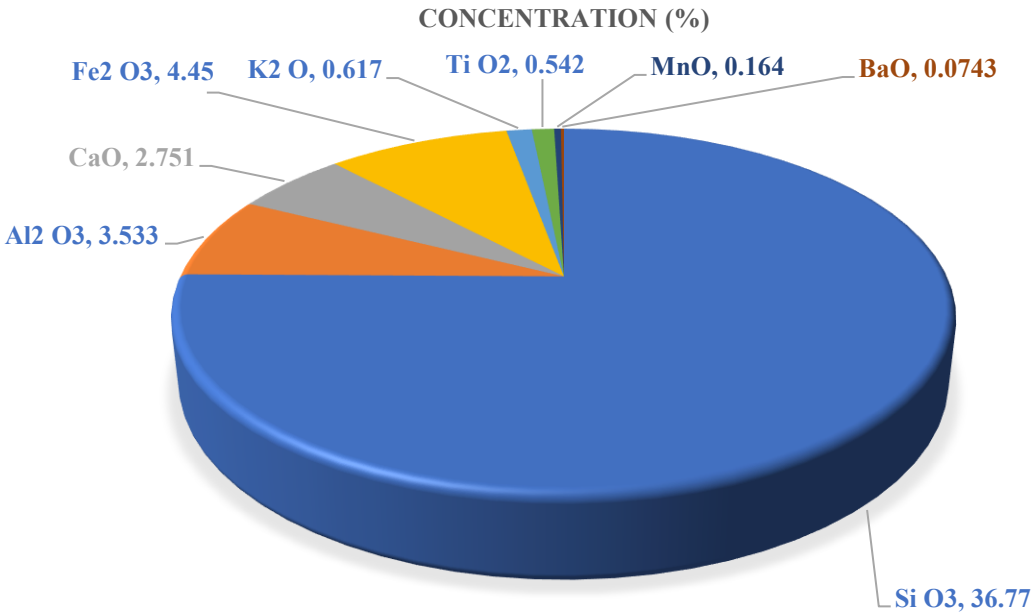

Figure 9 Chemical compound concentration of deposition samples.

The total and leached compositions were compared with the Rudnick and Gao [57] global average UCC. We included this comparison because the UCC is commonly used to determine lithogenic composition when local data sets are unavailable, and we aimed to demonstrate how Qassim PM varies from the UCC. The resolved data due to the chemical analysis of PM indicated that all the element concentrations were marginally greater than those published by Rudnick and Gao [49,57], with the exception of Al, As, Fe, Cr, Ba, Mn, and Ti. The highest concentrations were observed for Al, Fe, Ca, and K, which are considered the main components of PM. The basic elements were evident from the chemical analysis and accounted for most of the mass concentration of $PM_{2.5}$ and PM_{10}. The results of several samples, such as As, Pb, and Ti, indicated that they are not the main components in the particles given their very low concentrations. Atmospheric dust is a major contributor to particles in the Qassim region. The excess concentrations of several elements can be attributed to planktonic or anthropogenic sources. These elements had low concentrations in comparison with the UCC data, implying that their quantities in PM may be interpreted to be of dust origin. A similarity was observed in the concentrations of compounds compared with the UCC data except for SiO_2. Silica is a common component of sand in numerous parts of the world, and given that the majority of PM in Qassim originated from sandstorms, the SiO_2 level is significant.

The first set of elements, including Al, Fe, Cr, Ca, Mn, Ni, Pb, and Li, may be of dust origin. The second category consisted primarily of biogenic or anthropogenic elements, such as As, Ti, Cu, Mo, and Zn. Heavy metals have been found in settling dust samples. The study was able to investigate the types and sizes of minerals in a range of environments. The most likely metal sources were established using anthropogenic and high concentration variations (V, Cr, Cu, Ni, Zn, Pb, Br, and Mn) and geochemical analyses (K, Al, Ti, Fe Si, and Ca). With the combination of the 4 crustacean parts, the crustacean contribution in Qassim was rather substantial (Fe, K, Ca, and Al). Mg, 185 Ca, Al, K, and Fe components were frequently linked with specific sources such as manufacturing, agriculture, and unpaved roads.

The chemically examined deposition samples contained large quantities of SiO_2 (**Figure 9**) with an average of 36.7 % quartz, along with an average Al_2O_3 of 3.5 % and average CaO of 2.7 % in plagioclase. K_2O had an average of 0.617 % in potassium feldspars. The samples previously detected by XRD-SiO_2, Al_2O_3, Fe_2O_3, TiO_2, MnO, BaO, and several K_2O- also contained clay, mica, and amphiboles. Gypsum and calcite contained smaller concentrations of CaO with MgO in dolomite. The Fe in Fe_2O_3 can be found in the goethite $FeO(OH)Fe_2O_3$ or clay crystals, including illite. Significant fractions of iron in soils and contaminants have been proposed as amorphous, quartz, and feldspar colloidal coatings [58].

XRD analyses of the 23 samples (**Figure 10**) established the variable amounts of quartz (47 %), calcite (21.5 %), alpha-SiO_2 (8 %), dolomite (4.57 %), SiO_2 (3.29 %), mica (2.04 %), dissakisite-(Ce) (1.6 %),

annealed mineral (NR) (1.26 %), paragonite-2M1 (1.21 %), tin yttrium zinc (1.17 %), tripotassium manganate (1.01 %), and low quantities of (0.9 to 0.01 %) zirconium cerium oxide, phosphonium iodide, lutetium silicon, albite, calcian, hexamolybdate dihydrate, stolzite, lithium oxovanadium, calcium carbonate, barium calcium molybdenum, calcium sodium aluminum silicon oxide, lanthanum indium antimonide, dithallium, trioxoselenate, boron iron neodymium, and copper indium zirconium.

The proportion of quartz rose concurrently from 19 to 83 %, except for sample 4 (**Figure 10**). The calcite values rose from 9.8 to 52.5 %, except for samples 2, 3, 15, and 18. The mineral group of dolomites decreased from 25.9 to 6.6 % in all samples. The concentration of alpha-SiO_2 in the samples varied from 0 to 90 %. SiO_2 was present only on samples 18 and 21, with amounts of 51.4 and 24 %, respectively. Mica was present only on sample 21 at 47 %. Likewise, dissakisite-(Ce) (39 % in sample 6), NR (29 % in sample 1), paragonite-2M1 (28 % in sample 13), tin yttrium zinc (27 % in sample 15), and tripotassium manganate (23.3 % in sample 22) were detected in selected samples.

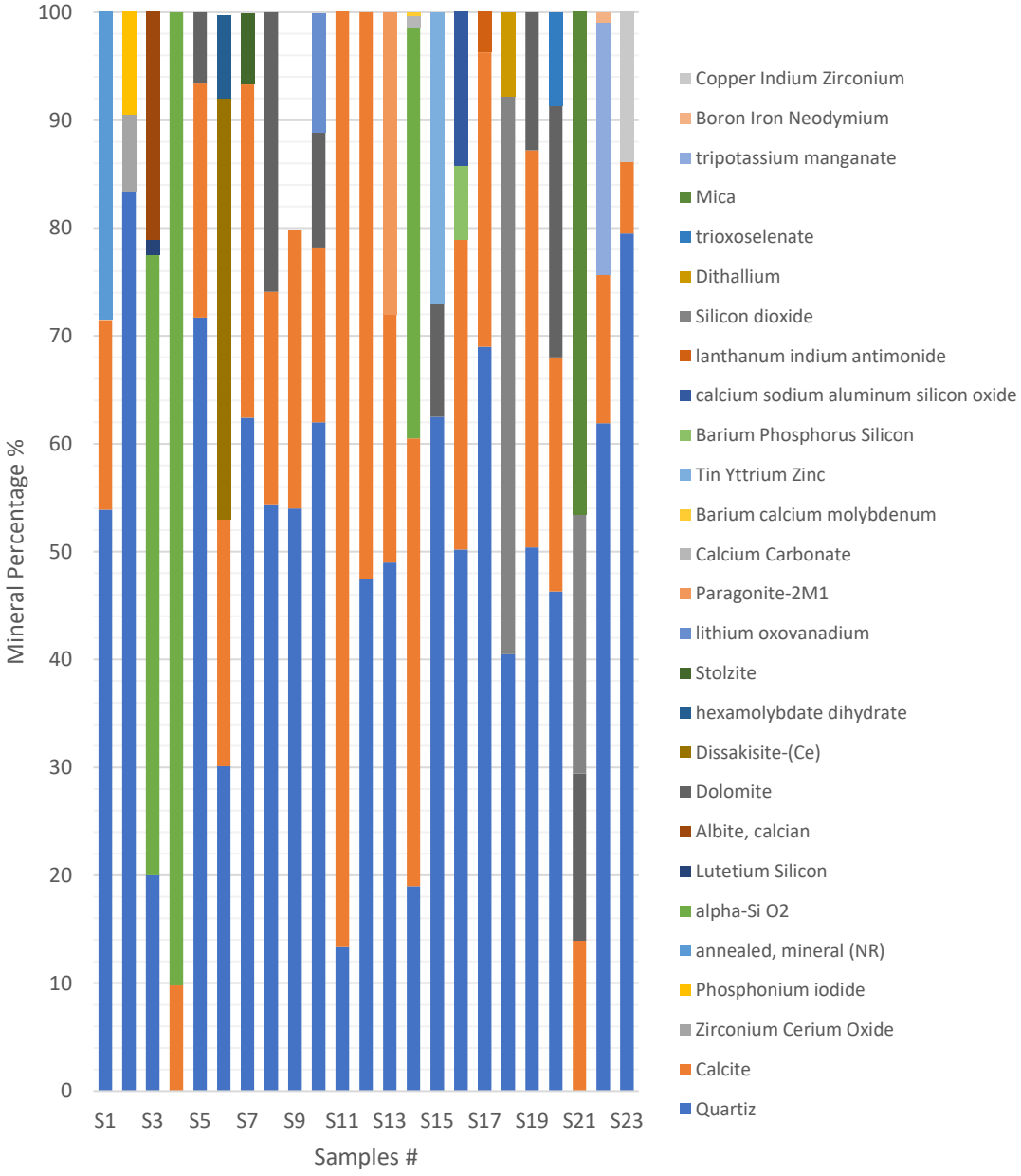

Figure 10 Chemical compound as minerals (%).

The XRD results of the dust samples were measured, and the XRD data were identical. **Figure 11** shows the XRD data for sample 1. Contrastingly, the intensity was averaged at the most extreme peak (2θ), and the peaks represented various minerals. The plot for 2θ value was in the range of 0 - 100 °.

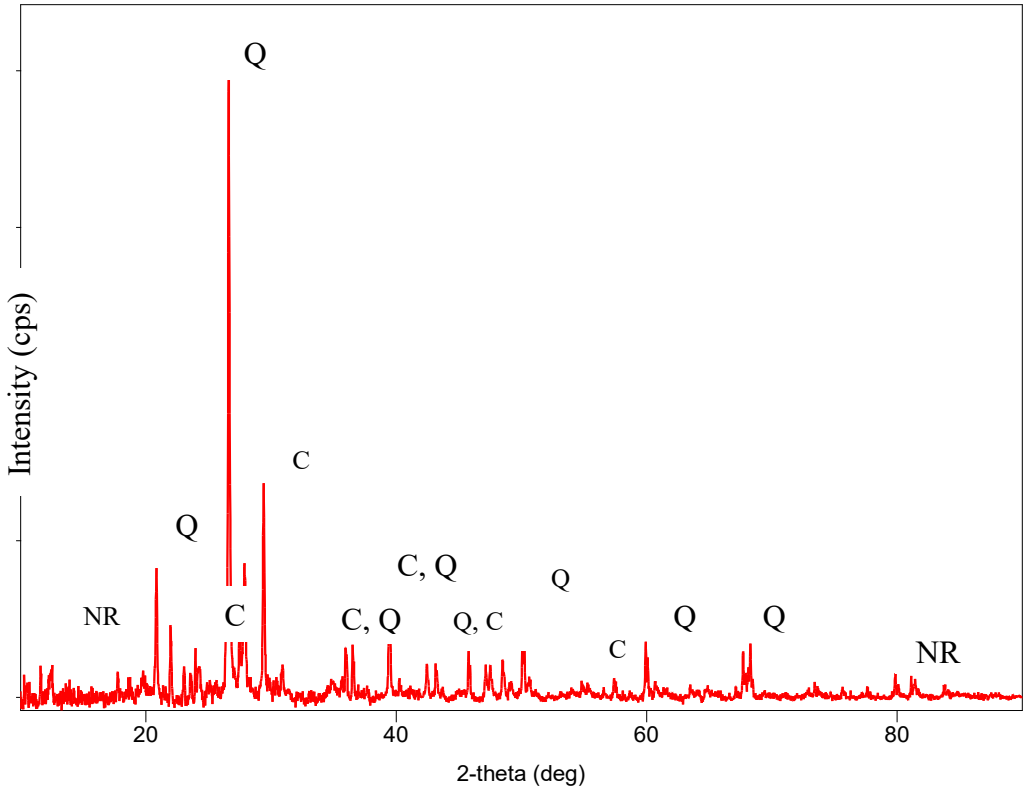

Figure 11 Measurement profile of sample 1.

Different letters reflect the peaks of numerous minerals: Q = quartz, C = calcite, and NR = annealed mineral. Minerals were detected in dust samples by contrasting the signature XRD peaks to those in literature and the RRUFF open-access reference database [59].

Finally, several components showed regular dependence on the PM concentration, which is in contrast to the typical seasonal variety caused by meteorology (high concentrations amid cold seasons with strong inversions).

Table 5 shows the results of EF calculation for various components. The EF results were compared with the regional findings provided by Ganor *et al.* [16]. The computed EFs were less than the equivalent values listed by Ganor *et al.* [16]. The EF findings varied from 0.2 to 59.3. According to the categories proposed by Ganor *et al.* [16], an EF less than 2 results in non-enriched elements, whereas an EF greater than 7 has a substantial influence on people and the environment (unhealthy). Meanwhile, EFs that are greater than 2 and less than 7 result in intermediately enriched elements. An investigation should be started to gather more information to determine the reason for the increased EF to prevent any negative effects on human and environment.

Out of the 18 elements, 6 were not enriched (Al, Be, Zr, As, K, Rb, Ti, and Mn), and their EF was less than 2. The elements with intermediate enrichment included V, Ni, Cr, Cu, Ca, Ba, Sr, and Pb, and their EF was greater than 2 and less than 7. Only Zn and Br were enriched because their EF was greater than 7. This finding may be attributed to the highly urbanized area and anthropological operations in Qassim region [60]. Electrolysis is used to recover bromine from natural bromine-rich brine resources in the United States, Israel, and China. Bromine, in the form of bromide, is found in all living organisms in trace levels. However, no biological role in humans is known. Bromine is irritating to the eyes and throat, and it causes severe sores when it comes into touch with the skin (61). The 2 main ores that contain zinc are calamine (zinc silicate) and zinc blende, both of which are found in abundance. zinc is extracted from its ores by crushing and roasting the ore, followed by reduction with carbon or electrolysis to produce zinc. Inhaling recently generated zinc (II) oxide can cause a condition known as the “oxide shakes” or “zinc chills” (62).

Table 5 Comparison of the EF with the regional and global weighted averages [57].

Elements	Current Study EF	Ganor *et al.* [16] (Fe, rock)
Al	0.8740176	NA
V	2.93741997	0.79
Ni	3.97419727	0.72
Cr	3.510004	1.01
Cu	5.65336779	0.6
Ca	3.43393919	NA
Zn	7.0878044	2.12
Zr	0.27886042	NA
As	1.97867873	2.25
K	0.63044798	NA
Br	59.3603618	4.69
Ba	2.23326032	1.03
Sr	2.46345502	1.25
Rb	1.50756474	0.82
Pb	4.84194324	4.66
Ti	1.12564834	NA
Mn	0.91095815	NA

Conclusions

In this work, we report the results of XRF and XRD analyses of 276 dust samples from 23 locations in Qassim Region, where we found the abundances of 18 elements and 8 compounds. According to the findings of the investigation, the concentration of PM_{10} and $PM_{2.5}$ was shown to be greater than the permitted level. The experimental findings showed that the average $PM_{2.5}$was considered unhealthy. Thus, humans must care for themselves and avoid outdoor activities on certain days. In addition, the windows and doors of houses must be closed during peak hours. Also, the finding confirmed that PM concentrations in spring and summertime (March to August) were higher than those in other seasons because of sandstorms, and the concentration is significantly higher in urban regions compared to rural areas. In this study, the most likely metal origin was determined by the anthropogenic and high-concentration (Cr, V, Cu, Zn, Ni, Pb, Mn, and Br) and geochemical (Al, Ca, Fe Si, K, and Ti) variants. The crustal source of Qassim's contribution was fairly high.

Acknowledgements

The authors gratefully acknowledge the use of the ED-XRF spectrometer and XRD at Universiti Sains Malaysia, Malaysia and Qassim University, Saudi Arabia for the analyses described in this paper.

References

[1] JA Bernstein, N Alexis, C Barnes, IL Bernstein, A Nel, D Peden and PB Williams. Health effects of air pollution. *J. Allergy Clin. Immunol.*2004; **114**, 1116-23.

[2] A Dondi, C Carbone, E Manieri, D Zama, CD Bono, L Betti, C Biagi and M Lanari. Outdoor air pollution and childhood respiratory disease: The role of oxidative stress. *Int. J. Mol. Sci.* 2023; **24**, 4345.

[3] D Fowler, K Pilegaard, MA Sutton, P Ambus, M Raivonen, J Duyzer, D Simpson, H Fagerli, S Fuzzi , JK Schjoerring, C Granier, A Neftel, ISA Isaksen, P Laj, M Maione, PS Monks, J Burkhardt, U Daemmgen, J Neirynck, E Personne and JW Erisman. Atmospheric composition change: Ecosystems-atmosphere interactions. *Atmos. Environ.* 2009; **43**, 5193-267.

[4] S Wang, Z Xie, R Wu and K Feng. 2022. How does urbanization affect the carbon intensity of human well-being? A global assessment. *Appl. Energ.* 2022; **312**, 118798.

[5] MM Mustafa, AE Behiry and YME Mossad. Al-Qassim industrial area and its role in changing the diseases patterns among workers over the past five years (2011 - 2015). *Int. J. Community Med. Publ. Health* 2016; **3**, 3465-73.
[6] National Center of Meteorology, Available at: https://ncm.gov.sa/ar/Pages/default.aspx, accessed December 2022.
[7] SR Nayebare, OS Aburizaiza, HA Khwaja, A Siddique, MM Hussain, J Zeb, F Khatib, DO Carpenter, and Blake. Chemical characterization and source apportionment of PM2.5 in Rabigh, Saudi Arabia. *Aerosol Air Qual. Res.* 2016; **16**, 3114-29.
[8] B Alharbi, MM Shareef and T Husain. Study of chemical characteristics of particulate matter concentrations in Riyadh, Saudi Arabia. *Atmos. Pollut. Res.* 2015; **6**, 88-98.
[9] S Munir, TM Habeebullah, AM Mohammed, EA Morsy, M Rehan and K Ali. Analysing PM2.5 and its association with PM10 and meteorology in the arid climate of Makkah, Saudi Arabia. *Aerosol Air Qual. Res.* 2017; **17**, 453-64.
[10] VH Garrison, EA Shinn, WT Foreman, DW Griffin, CW Holmes, CA Kellogg, MS Majewski, LL Richardson, B Ritchie and GW Smith. African and Asian dust: From desert soils to coral reefs. *BioScience* 2003; **53**, 469-80.
[11] AA Al-Taani, M Rashdan and S Khashashneh. Atmospheric dry deposition of mineral dust to the Gulf of Aqaba, Red Sea: Rate and trace elements. *Mar. Pollut. Bull*. 2015; **92**, 252-8.
[12] R Zhang, R Arimoto, J An, S Yabuki and J Sun. Ground observations of a strong dust storm in Beijing in March 2002. *J. Geophys. Res. Atmos.* 2005; **110**, D18S06.
[13] LR Crilley, F Lucarelli, WJ Bloss, RM Harrison, DC Beddows, G Calzolai, S Nava, G Valli, V Bernardoni and R Vecchi. Source apportionment of fine and coarse particles at a roadside and urban background site in London during the 2012 summer ClearfLo campaign. *Environ. Pollut.* 2017; **220**, 766-78.
[14] S Kundu and EA Stone. Composition and sources of fine particulate matter across urban and rural sites in the Midwestern United States. *Environ. Sci. Process. Impacts* 2014; **16**, 1360-70.
[15] PJ Borm, F Kelly, N Künzli, RP Schins and K Donaldson. Oxidant generation by particulate matter: From biologically effective dose to a promising, novel metric. *Occup. Environ Med.* 2007; **64**, 73-4.
[16] E Ganor, HA Foner, S Brenner, E Neeman and N Lavi. The chemical composition of aerosols settling in Israel following dust storms. *Atmos. Environ. A* 1991; **25**, 2665-70.
[17] SM Awadh. Impact of North African sand and Dust storms on the Middle East using Iraq as an Example: Causes, sources, and mitigation. *Atmosphere* 2023; **14**, 180.
[18] JM Al-Awadhi, AM Al-Dousari and FI Khalaf. Influence of land degradation on the local rate of dust fallout in Kuwait. *Atmos. Clim. Sci.* 2014; **4**, 437-46.
[19] AM Al-Dousari. *Recent studies on dust fallout within preserved and open areas in Kuwait*. *In*: NR Bhat, AY Al-Nasser and SAS Omar (Eds.). Desertification in arid lands. Institute for Scientific Research, Kuwait City, Kuwait, 2009, 137-47.
[20] AM Al-Dousari, A Aba, S Al-Awadhi, M Ahmed and N Al-Dousari. Temporal and spatial assessment of pollen, radionuclides, minerals and trace elements in deposited dust within Kuwait. *Arab. J. Geosci.* 2016; **9**, 95.
[21] E Al-enezi, A Al-Dousari and F Al-shammari. Modeling adsorption of inorganic phosphorus on dust fallout in Kuwait bay. *J. Eng. Res.* 2014; **2**, 1.
[22] N Subramaniam, M Al-Sudairawi, A Al-Dousari and N Al-Dousari. Probability distribution and extreme value analysis of total suspended particulate matter in Kuwait. *Arab. J. Geosci*. 2015; **8**, 11329-44.
[23] AA Al-Taani, Y Nazzal and FM Howari. Assessment of heavy metals in roadside dust along the Abu Dhabi-Al Ain National Highway, UAE. *Environ. Earth Sci*. 2019; **78**, 411.
[24] J Dan. The effect of dust deposition on the soils of the land of Israel. *Quaternary Int.* 1990; **5**, 107-13.
[25] E Ganor and Y Mamane. Transport of Saharan dust across the eastern Mediterranean. *Atmos. Environ.* 1982; **16**, 581-7.
[26] S Norouzi, H Khademi, AF Cano and JA Acosta. Using plane tree leaves for biomonitoring of dust borne heavy metals: A case study from Isfahan, Central Iran. *Ecol. Indicat.* 2015; **57**, 64-73.
[27] AA Shaltout, MI Khoder, AA El-Abssawy, SK Hassan and DLG Borges. Determination of rare earth elements in dust deposited on tree leaves from Greater Cairo using inductively coupled plasma mass spectrometry. *Environ. Pollut.* 2013; **178**, 197-201.

[28] F Amato, M Pandolfi, A Escrig, X Querol, A Alastuey, J Pey and PK Hopke. Quantifying road dust resuspension in urban environment by multilinear engine: A comparison with PMF2. *Atmos. Environ.* 2009; **43**, 2770-80.
[29] SJ Blott, AM Al-Dousari, K Pye and SE Saye. Three-dimensional characterization of sand grain shape and surface texture using a nitrogen gas adsorption technique. *J. Sediment. Res.* 2004; **74**, 156-9.
[30] SM Doronzo and A Al-Dousari. Preface to dust events in the environment. *Sustainability* 2019; **11**, 628.
[31] MP Fraser, ZW Yue and B Buzcu. Source apportionment of fine particulate matter in Houston, TX, using organic molecular markers. *Atmos. Environ.* 2003; **37**, 2117-23.
[32] Ministry of Interior, Saudi Arabia's national unified portal for government services, Available at: https://www.my.gov.sa/wps/portal/snp/main, accessed December 2022.
[33] Climate and average weather year round in Buraydah Saudi Arabia, Available at: https://weatherspark.com/y/102734/Average-Weather-in-Buraydah-Saudi-Arabia-Year-Round, accessed December 2022.
[34] H Alnagran, S Alashrah, N Suardi and H Mansour. Study of radionuclides and assessment of radioactive risks for environmental particulate matters in Qassim region, Saudi Arabia. *Pollution* 2022; **8**, 1049-60.
[35] Google maps. Al Qassim Province, Available at: https://maps.google.com, accessed May 2023.
[36] Meteoblue. Weather archive Buraidah, Available at: https://www.meteoblue.com/en/weather/historyclimate/weatherarchive/buraidah_saudi-arabia_107304?fcstlength=1y&year=2023&month=5, accessed May 2023.
[37] A Valavanidis, K Fiotakis and T Vlachogianni. Airborne particulate matter and human health: Toxicological assessment and importance of size and composition of particles for oxidative damage and carcinogenic mechanisms. *J. Environ. Sci. Health C* 2008; **26**, 339-62.
[38] M Yang, HX Zeng, XF Wang, H Hakkarainen, A Leskinen, M Komppula, M Roponen, QZ Wu, SL Xu, LZ Lin and RQ Liu. Sources, chemical components, and toxicological responses of size segregated urban air PM samples in high air pollution season in Guangzhou, China. *Sci. Total Environ.* 2023; **865**, 161092.
[39] SM McLennan. Relationships between the trace element composition of sedimentary rocks and upper continental crust. *Geochem. Geophys. Geosyst.* 2001; **2**, 2000GC000109.
[40] GMS Abrahim and RJ Parker. Assessment of heavy metal enrichment factors and the degree of contamination in marine sediments from Tamaki Estuary, Auckland, New Zealand. *Environ. Monit. Assess*. 2008; **136**, 227-38.
[41] J Lv, Y Liu, Z Zhang, R Zhou and Y Zhu. Distinguishing anthropogenic and natural sources of trace elements in soils undergoing recent 10-year rapid urbanization: A case of Donggang, Eastern China. *Environ. Sci. Pollut. Res.* 2015; **22**, 10539-50.
[42] RL Rudnick and S Gao. *The crust*: *Treatise on geochemistry*. Elsevier, Amsterdam, Netherlands, 2014.
[43] D Rojas-Rueda, W Alsufyani, C Herbst, S AlBalawi, R Alsukait and M Alomran. Ambient particulate matter burden of disease in the Kingdom of Saudi Arabia. *Environ. Res.* 2021; **197**, 111036.
[44] M Alwadei, D Srivastava, MS Alam, Z Shi and WJ Bloss. Chemical characteristics and source apportionment of particulate matter (PM2.5) in Dammam, Saudi Arabia: Impact of dust storms. *Atmos. Environ. X* 2022; **14**, 100164.
[45] SR Nayebare, OS Aburizaiza, A Siddique, DO Carpenter, MM Hussain, J Zeb, AJ Aburiziza and HA Khwaja. Ambient air quality in the holy city of Makkah: A source apportionment with elemental enrichment factors (EFs) and factor analysis (PMF). *Environ. Pollut.* 2018; **243**, 1791-801.
[46] M Khodeir, M Shamy, M Alghamdi, M Zhong, H Sun, M Costa, LC Chen and P Maciejczyk. Source apportionment and elemental composition of PM2.5 and PM10 in Jeddah City, Saudi Arabia. *Atmos. Pollut. Res.* 2012; **3**, 331-40.
[47] W Farah, MM Nakhlé, M Abboud, N Ziade, I Annesi-Maesano, R Zaarour, N Saliba, G Germanos, NA Saliba, AL Shihadeh and J Gerard. Analysis of the continuous measurements of PM 10 and PM 2.5 concentrations in Beirut, Lebanon. *Environ. Eng. Manag. J.* 2018; **17**, 1693-700.
[48] W Javed, M Iakovides, EG Stephanou, JM Wolfson, P Koutrakis and B Guo. Concentrations of aliphatic and polycyclic aromatic hydrocarbons in ambient PM2.5 and PM10 particulates in Doha, Qatar. *J. Air Waste Manag. Assoc.* 2019; **69**, 162-77.
[49] M Adam. Suspended particulates concentration (PM10) under unstable atmospheric conditions over subtropical urban area (Qena, Egypt). *Adv. Meteorol*. 2013; **2013**, 457181

[50] RA Eldred, TA Cahill and RG Flocchini. Composition of PM2.5 and PM10 aerosols in the IMPROVE network. *J. Air Waste Manag. Assoc.* 1997; **47**, 194-203.
[51] X Querol, A Alastuey, CR Ruiz, B Artiñano, HC Hansson, RM Harrison, E Buringh, HM ten Brink, M Lutz, P Bruckmann, P Straehland and J Schneider. Speciation and origin of PM10 and PM2.5 in selected European cities. *Atmos. Environ.* 2004; **38**, 6547-55.
[52] World Health Organization. *Air quality guidelines: Global update 2005.* Druckpartner Moser, Rheinbach, Germany, 2006.
[53] Ministry of Health Saudi Arabia, Available at: https://www.moh.gov.sa/en/Pages/default.aspx, accessed May 2023.
[54] LL Tang, SJ Niu, SX Fan, H Nie, RX Gao, SH Jin and GY Yang. Observational study of spectral distribution of polycyclic aromatic hydrocarbons (PAHs) and PM10 in Waliguan and Xining. *Plateau Meteorol* 2010; **29**, 236-43.
[55] JS Apte, JD Marshall, AJ Cohen and M Brauer. Addressing global mortality from ambient PM2. 5. *Environ. Sci. Tech*. 2015; **49**, 8057-66.
[56] J Chen and G Hoek. Long-term exposure to PM and all-cause and cause-specific mortality: A systematic review and meta-analysis. *Environ. Int.* 2020; **143**, 105974.
[57] RL Rudnick, S Gao, HD Holland and KK Turekian. Composition of the continental crust. *Treatise Geochem.* 2003; **3**, 1-64.
[58] JP Engelbrecht, H Moosmüller, S Pincock, RKM Jayanty, T Lersch and G Casuccio. Mineralogical, chemical, morphological, and optical interrelationships of mineral dust re-suspensions. *Atmos. Chem. Phys.* 2016; **16**, 10809-30.
[59] B Lafuente, RT Downs, H Yang, N Stone, T Armbruster and RM Danisi. *Highlights in mineralogical crystallography*. De Gruyter, Berlin, Germany, 2015, p. 1-30.
[60] JV Jones III, NM Piatak and GM Bedinger. *Zirconium and hafnium*. US Geological Survey, Virginia, 2017
[61] JA Puccio. *Halogens*. *In*: RD Harbison, MM Bourgeois, GT Johnson. Hamilton & Hardy's industrial toxicology. John Wiley & Sons, New Jersey, 2015, p. 341-56.
[62] D Sadananda, AMM Mallikarjunaswamy, CN Prashantha, R Mala, K Gouthami, L Lakshminarayana, LFR Ferreira, M Bilal, A Rahdar and SI Mulla. Recent development in chemosensor probes for the detection and imaging of zinc ions: A systematic review. *Chem. Papers* 2022; **76**, 5997-6015.